OPTIMAL DESIGN OF TAPER ROLLER BEARING ARRANGEMENTS. PART I: OBJECTIVE FUNCTION

LUCIAN TUDOSE[1,2], SIMION HARAGÂŞ[1], CRISTINA TUDOSE[2],
NICOLETA PREDELEANU[1], COSTEL URSACHE[1]

Abstract. Contrasting previous works in this peculiar field, where bearing rolling elements deformations are regarded as the result of known loads – most likely obtained from the shaft static equilibrium, neglecting the bearing deformations – a system approach conveying ineluctably different results is thereby proposed. The method is grounded on a straightforward theory: when the static equilibrium of the shaft is reached, the loads and moments transmitted from the shaft to the bearings must be balanced by the loads and moments arisen due to the elastic deformations of the rolling elements. In this approach, the formers are obtained using the slope-deflection method, whereas the latter may result from a deformation model of rolling elements of the bearing. The succeeding part of the paper render the precise use of the method broached, mirrored in life calculations of the bearings of particular arrangements. The optimal design of a bearing arrangement (from the maximum bearing lives standpoint) is ultimately illustrated.

Key words: bearing loads, slope-deflection method, taper roller bearings.

1. INTRODUCTION

Regardless of the method applied (e.g. following ISO 281 [22] or ISO 16281 [23]), the prediction accuracy of bearing rating life depends on the values of the loads and moments acting on the bearing, used as input data in the calculation. Considering the shaft on which the bearings are mounted a statically loaded beam, with the external loads and bending moments originating from the machine elements mounted on the shaft, is a current practice. The supports of this beam are the bearings mounted on the shaft, case in which the values of loads and tilting moments acting on the bearings are equal to the values of the support reactions and reaction moments. It was proved that the bearing load calculation, considering the shaft resting on totally rigid supports could lead to severe mistakes in bearing life calculations. Undoubtedly, for a correct calculation of the bearing loads, the supports must be considered deformable, as they are indeed, which eventually leads to a systemic approach.

[1] Technical University of Cluj-Napoca, Romania
[2] RKB Bearing Industries, Balerna, Switzerland

Ro. J. Techn. Sci. – Appl. Mechanics, Vol. 62, N° 3, P. 218–241, Bucharest, 2017

The problem is complicated, hence solving it cannot possibly be imagined today without massive FE analysis; without any doubt, the extremely high difficulty of the problem requires an extraordinarily efficacious tool to solve it. An eloquent example would be the SYBER program [21], a sophisticated tool, capable of analyzing a full system, with several shafts, bearings, gears, and housings. But it should certainly be used for very special and important projects, and in the last stages of the design, when the actual design solution is closed to the definitive one. In the early stages of a machine design, the need of a fast and reliable tool to estimate bearing lives is strongly felt, even if this instrument is encumbered by some inherent simplifications or approximations. This tool has to be based on an as accurately as possible calculation of the bearing loads by considering the shaft supports as deformable. The aim of the first part of this paper is to advance a new bearing load calculation method. The subsequent constituent sections specify its concrete usage in life calculations of the bearings of certain arrangements; lastly, the optimal design of an arrangement (from the perspective of the maximum bearing lives) is highlighted.

The concept lying behind the suggested method is elementary: when the static equilibrium of the shaft is reached, the loads and moments transmitted from the shaft to the bearings must be balanced by the loads and moments arisen due to the elastic deformations of the rolling elements. In the proposed approach, the formers are obtained using the slope-deflection method, and the latter result from a certain load-deformation model of rolling elements of the bearing. Thus, the primary unknowns are the displacements of the shaft support reference points which are determined first by solving the equations of equilibrium. Once these displacements are found, the unknown forces are obtained through compatibility considerations and force–displacement relations.

2. SLOPE-DEFLECTION METHOD AND BEARING DEFORMATION MODELS

The slope-deflection method was originally developed in the late nineteenth century when, for simple trusses, engineers attempted first to solve the pin-jointed behavior and only then, in a second stage, to add the effect of joint rotations (called at a time *secondary stresses*). Such a complex calculation proposing an iterative solution to the equations set (with joint rotations as unknowns) was first published by Manderla in 1880 [32]. A real milestone in the development of the theory of secondary stresses was the work of Mohr, from 1892–1893 [36], where he introduced and upgraded the version of Manderla's method. Twelve years later, the Danish engineer, Bendixsen, extended Mohr's procedure to braced and sway frames [4]. One year later, in 1915, probably unaware of Bendixsen's work, Wilson and Maney [42] developed a refined version of this technique (which was not dissimilar to Bendixsen's method) and applied it to the analysis of indeterminate beams and framed structures. It is very likely that the name of the method (accepted even nowadays) had been given by the analysis [43] of Wilson *et al*.

published in 1918, rather than that from 1915. Referring to a statically indeterminate structure, all the analyses in this bulletin are based upon the following assumptions: (1) the connections are perfectly rigid; (2) the length of a member is not changed by axial stress; (3) the shearing deformation is zero. It is uncomplicated to notice that each of these assumptions perfectly matches the loaded shafts used in mechanical applications. One of the first comprehensive descriptions of the slope deflection method can be found in [34].

Today, being applicable to a large category of 2D and 3D structures with straight or curved, deformable or infinitely rigid members, the slope-deflection method is a highly competent instrument in structural analysis. Virtually, there is no reliable book in this field that does not approach the subject. Without any preference in mind, for further information, the reader is advised to address one of the following modern books [5, 19, 26, 29, 33, 35]; and the enumeration could have been continued.

After Sjoväll's pioneering work [40], probably the first general equations for the elastic equilibrium of a ball bearing in three of the five possible degrees of freedom were given by Jones in 1946 [24]. Several years later he has brilliantly completed his work [25] and a general model was issued, whereby the elastic compliances of a system of any number of ball and radial roller bearings under any system of loads can be determined. The system approach signifies that the entire assemblage of bearings, shaft, and supporting structure was looked at as a single, elastic system. The solution defines the elastic compliance of a point on the shaft with respect to the supporting structure in five degrees of freedom. Considering also the centrifugal forces and gyroscopic moments acting on the rolling elements, the internal load distribution is determined for all the bearings in the system. Finally, bearing lives are evaluated by summation of the fatigue effects of the passages of the rolling elements over precisely determined paths in each bearing raceway. It is worth noting here that the shaft and supporting structure deflections and slopes are related to the shaft reference line through influence coefficients and all as functions of external loading of the shaft. It must have been the complexity and high degree of difficulty of the approach that triggered, decades after the publication of these studies, the focus of most researchers on developing models in which the bearing inner loads distribution is obtained from the known external loads, taking into account the variation in the contact angle with the loading conditions. Several such examples will hereinafter be provided, in chronological order.

In a theoretical analysis, regarding the dynamics of ball bearings [14] and in its associated paper encompassing the numerical results of the dynamic simulations [15] Gupta presents a general interaction model – formulated for arbitrary but known external loads – on a ball bearing. Analytical framework for the computation of the applied force and moment vectors due to ball-race and ball-cage interactions, are described in adequate detail. According to this approach, the formulation of ball-race interaction can be divided into three parts: (1) definition of the different position vectors and formulation of relevant geometrical interactions; (2) computation of the normal contact force between balls and raceways, using the

conventional Hertzian elastic contact theory; (3) formulation of the slip velocity vectors and traction force vectors for a given traction model. Detailing, since the main target is this one, the normal contact forces are primarily determined by first locating the ball relative to the race and computing the deflection at the point of interaction and then using the Hertzian point contact solutions to obtain the load-deflection relationship. A similar approach was applied to cylindrical roller bearings ([12] and [13], respectively).

In a two-part work, De Mul et al. constructed a general mathematical model for the calculation of the equilibrium and associated load distribution in both ball [7] and roller bearings [8]. The bearings may be loaded – with known loads and moments – and displaced in five degrees of freedom. The analysis is made with and without considering the centrifugal forces, acting on the rolling elements, whilst the internal friction is neglected. The material is assumed linearly elastic and the bearing rings are modelled as rigid, except for the local contact deformation. In order to formulate the rolling element compressive loads either classical Hertzian contact analysis or non-Hertzian line contacts (extended technique, utilized today, involving the roller slicing in a large number of laminae) is used.

In order to derive a bearing stiffness model for vibration transmission analysis Lim and Singh [30] had to establish the relationships between the known bearing loads and moments transmitted through the rolling element bearing, and the bearing displacements in 5 DOF. As in the modern models, for ball bearings, they used the variation of the unloaded and loaded relative distances between the inner and outer raceway groove curvature centers, in ball deformation calculation. Unfortunately, though, this model is not concerned with the centrifugal forces that act on the balls of the high-speed ball bearings. Eventually, a bearing stiffness matrix suitable for the analysis of the vibration transmission through either ball or roller bearings is determined. The reader could find more details in the authors' previous work [39]. In 2012, Gunduz [10] continued this work and developed the formulation of the stiffness matrix for a double-row angular ball bearing.

Houpert [20] proposed a so-called "uniform analytical approach" for ball and roller bearings which provides simple analytical equations to calculate the bearing loading (three loads and two tilting moments) based on the bearing raceway relative displacements (5 DOF). He called this approach "uniform" by virtue of the fact that the equations obtained for the rolling element deformation are exactly the same, both for radial ball and roller bearings, when the variation of the contact angle under load is neglected. In a subsequent analysis, this approximation is removed. The interesting component of this approach is the manner of introducing the so-called "equivalent displacements" and expressing the rolling element-race load as a function of them. Moreover, the three components of the load and the two components of the moment on the inner raceway are calculated by integration, not by discrete summation. In 2014, Houpert strongly enhanced his model [21], especially for roller bearings.

Hernot *et al*. [18] presented two stiffness matrices of angular contact ball bearings. Using the two leading Sjoväll's load-distribution integrals J_a and J_r, the

summation of ball-raceway loads was replaced by an integration and, in this way, the matrix connected to the conventional model in 2 DOF is first introduced. Using the constructed model, a study of a two bearing-shaft assembly where shaft deformations are ignored, was carried out. But, by taking preload into account it was clearly demonstrated how the influence of the preload on the assembly rigidity and bearing fatigue life may be analyzed. Conclusively, the matrix formulation of the 5 DOF model, connected with the Houpert's early model [20], is presented.

In two successive papers, Liao and Lin established [27] and then developed [28] a tree-dimensional expression for the elastic deformation of bearing balls in terms of the geometry of the contact surface and the inner and outer raceways positions. The main contribution they claimed was that the contact angle was not considered constant, but variable with the position of each ball. But, in fact, the variability of the contact angle was looked at, invoking Jones's mentioned works. The geometrical analysis is engaging and valuable, but the bearing was treated as loaded with radial and axial loads (no tilting moments) and only the radial and axial displacement of raceways were taken into account (no rotations).

Bai and Xu [2] reported a dynamic model of ball bearings used to study the dynamic properties of a rotor system supported by ball bearings under the effect of both internal clearance and raceway waviness. The proposed model includes centrifugal forces and gyroscopic moments. For the relationship between the ball displacement vector and the displacement vector of the bearing center they used the same transformation matrix as De Mul [7], but to the ball displacement vector, a vector containing the relative waviness of the inner and outer raceway is added. Once more, the equilibrium is reached for a given set of external loads and moments. In a successive paper, Bai *et al*. [3] used the same model for the same purpose, with no reference to the waviness effect this time.

Relative to our preeminent topic, in the fundamental two-volume monograph, Harris and Kotzalas presented either the Sjoväll's model of load distribution within ball and roller bearings under given external radial and axial load [16], or, partially [17], the Jones's already mentioned work.

In order to determine the effect of the bearing internal clearance or interference on the load distribution among the rolling elements and on the life of (only) radially loaded deep-groove ball bearings and cylindrical roller bearings, Oswald *et al*. [38] engaged three models: (1) computer analysis method: for a given set of two perpendicular radial loads, two radial inner-race displacements are calculated iteratively using the summation of each rolling element load; (2) load integral method: calculation of the maximum rolling-element load by using the load-distribution integral J_r augmented with additional data from Houpert [20]; (3) alternative method: calculation of the maximum rolling-element load using an iterative procedure to find the Striebeck Number (ratio between the maximum and the average ball or roller loads).

Recent works are focused on obtaining the bearing stiffness matrix by extending the Jones's approach as Noel *et al*. [37] or by using FEM as Guo and Parker [11]. In both approaches, the external bearing loading has to be known.

Relevant results were issued in the latter quoted paper, regarding the bearing radial and axial stiffness, respectively, the obtained radial/axial stiffness-load relationship for both radial cylindrical roller and ball bearings being significantly different from those predicted by Gargiulo's well-known equations (perhaps because these old equations did not take into account the elasticity of bearing rings). It is also interesting that they suggested, as previously Houpert did [20], that the load-deflection exponent for the line contact of a roller bearing is slightly different from the accepted value of 10/9.

As for the dynamic models of bearings, (even if it is focused on the spindle-bearing systems of machine tools) the reader can find a captivating review in [31].

3. REAL LOADS AND MOMENTS ACTING ON ROLLING BEARINGS

In order to determine the real values of the loads and moments acting on a bearing, one has envisage that a bearing could be assimilated with a set of Z spatial arranged springs (the Z rolling elements of the bearing) each having a non-linear characteristic. In our approach, the housing and the bearing rings are considered completely rigid (stiff), the only deformable parts being the rolling elements. The fundamental concept underlying the proposed procedure to determine the real loads acting on a bearing is: the loads and moments acting on the bearing should be equal to the loads and moments produced by elastic deformations of the rolling elements. Maintaining the general principle, the case of a shaft supported by two taper roller bearings (Fig. 1) will be hereinafter examined.

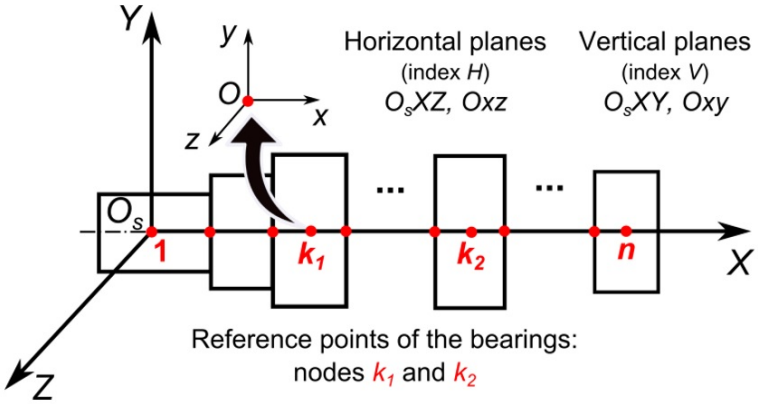

Fig. 1 – Cartesian global and local systems of coordinates referring to the shaft and bearings.

3.1. LOADS AND MOMENTS TRANSMITTED FROM THE SHAFT TO THE BEARINGS

In a previous work [41], it was proved that the vector of all loads and moments transmitted from the shaft to the bearings.

$$\mathbf{FM} = \left(\mathcal{F}_x \;\; \mathcal{F}_{yk_1} \;\; \mathcal{F}_{zk_1} \;\; \mathcal{M}_{yk_1} \;\; \mathcal{M}_{zk_1} \;\; \mathcal{F}_{yk_2} \;\; \mathcal{F}_{zk_2} \;\; \mathcal{M}_{yk_2} \;\; \mathcal{M}_{zk_2} \right)^{\mathrm{T}} \tag{1}$$

will be given by the equation:

$$\mathbf{FM} = \mathbf{A} \cdot \Delta\boldsymbol{\theta} + \mathbf{B} + \mathbf{FA} \tag{2}$$

where the components of the vector **FM** are the axial load $\mathcal{F}_x$ and the loads and moments acting in the nodes k_1 and k_2, respectively, (the reference points of the two bearings), **A** and **B** matrices derived from on the stiffness matrix of the shaft,

$$\mathbf{FA} = \left(F_a \;\; 0 \;\; 0 \;\; 0 \;\; 0 \;\; 0 \;\; 0 \;\; 0 \;\; 0 \right)^{\mathrm{T}} \tag{3}$$

(where F_a is the resulting external axial load acting on the shaft) and the unknown vector.

$$\mathbf{\Delta\Theta} = \left(\delta_x \;\; \delta_{yk_1} \;\; \delta_{zk_1} \;\; \theta_{yk_1} \;\; \theta_{zk_1} \;\; \delta_{yk_2} \;\; \delta_{zk_2} \;\; \theta_{yk_2} \;\; \theta_{zk_2} \right)^{\mathrm{T}}. \tag{4}$$

Has as components the displacements (δ_x – the same for both nodes, δ_y and δ_z – specific for each reference node) and rotations (θ_y and θ_z – specific also for each reference node).

Some comments would be required here. Matrices **A** and **B** are easily computable and their dimensions depend only on the number of bearings: **A** depends only on the shaft (geometry and material), and **B** depends on the shaft and its loading. All these transform this computation into a facile one, no matter how complicated the shape of the shaft and its loading is. It is worth remarking that the calculation of the reactions (loads and moments) on the shaft, as well as the deflections and rotations in nodes, becomes manageable and fast, regardless of the number and types of supports and no howbeit complicated the shaft shape would be.

3.2. LOADS AND MOMENTS TRANSMITTED TO THE SHAFT DUE TO THE ELASTIC DEFORMATIONS OF THE BEARING ROLLERS

For the rolling bearing analysis, one can consider the relative movement between the bearing rings. Referring to one bearing, all externally applied loads and moments and the displacements of the inner ring as well are in relation to a point on the inner ring axis of symmetry (bearing reference point-see also Fig. 1). According to Newton's Third Law, the bearing loading and the loading from the rolling elements on the inner ring raceway, both considered in the bearing reference point, should be cancelled. The objective of this section is to establish the relationship between the reaction loading and the displacements of the inner ring.

In order to limit the model complexity and following the most frequently used shafts, housings, and bearing arrangements, the ensuing assumptions are emphasized:

– Deformations of the shaft, housing and bearing rings are neglected and only the elastic deformations of the rolling elements are included.

– Centrifugal forces acting on the rolling elements, loads generated by interaction from the cage, frictional forces inside the bearings, and gyroscopic moments are neglected.

– Spring constants of the rollers are equal and constant with temperature.

Two coordinate systems were introduced, to facilitate the analysis in the bearing reference point: a right-handed Cartesian one ($Oxyz$, in both Fig. 1 and Fig. 2) and a cylindrical system $Or\varphi x$, where φ is the angle between the r-axis and positive y-direction, being positive if measured as depicted in Fig. 2.

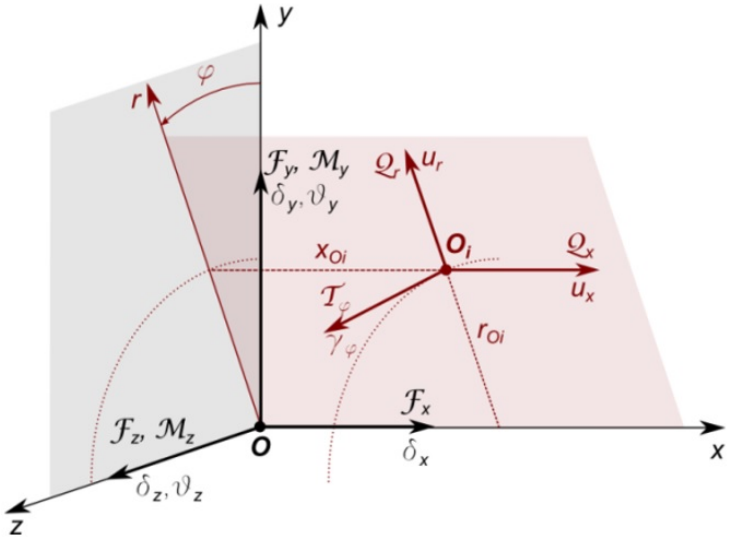

Fig. 2 – Bearing Cartesian and cylindrical coordinate systems. Inner ring loading and displacements.

Let the inner ring loading and displacement vectors be symbolized by $\boldsymbol{\mathcal{FM}}$ and $\boldsymbol{\delta\theta}$, respectively, and let the denotation of the loading from the rolling elements on the inner ring be $\boldsymbol{\mathfrak{fm}}$. All loads and displacements refer to the bearing reference point

$$\boldsymbol{\mathcal{FM}} = \left(\mathcal{F}_x \;\; \mathcal{F}_y \;\; \mathcal{F}_z \;\; \mathcal{M}_y \;\; \mathcal{M}_z\right)^{\mathrm{T}} \tag{5}$$

$$\boldsymbol{\delta\theta} = \left(\delta_x \;\; \delta_y \;\; \delta_z \;\; \theta_y \;\; \theta_z\right)^{\mathrm{T}} \tag{6}$$

$$\boldsymbol{\mathfrak{fm}} = \left(\mathfrak{f}_x \;\; \mathfrak{f}_y \;\; \mathfrak{f}_z \;\; \mathfrak{m}_y \;\; \mathfrak{m}_z\right)^{\mathrm{T}}. \tag{7}$$

Now, considering an inner ring axial section, positioned to such angle φ chosen so that the rx-plane passes through the reference point of the roller, being selected. As can be noticed, the analysis can be conducted by choosing the intersection point of the perpendiculars to the middle of the useful portion of opposite profiles of the roller (Fig. 2) as reference point of the selected inner ring axial section [6, 8, 20, 21]. This point will be stored as the following vector (relative to a Cartesian system of coordinates originated on the bearing axis of symmetry at its mid-width):

$$\mathbf{O}_i = \begin{pmatrix} r_{O_i} & x_{O_i} \end{pmatrix}^{\mathrm{T}}. \tag{8}$$

The above mentioned inner ring axial section is loaded (due to the roller deformation) in its reference point O_i by the load vector $\mathcal{QT}$:

$$\mathcal{QT} = \begin{pmatrix} \mathcal{Q}_r & \mathcal{Q}_x & \mathcal{T}_\varphi \end{pmatrix}^{\mathrm{T}} \tag{9}$$

with the displacement vector $\mathbf{u\gamma}$

$$\mathbf{u\gamma} = \begin{pmatrix} u_r & u_x & \gamma_\varphi \end{pmatrix}^{\mathrm{T}}. \tag{10}$$

Obviously, it is more convenient to consider another local system of coordinates $\xi\eta\zeta$ (Fig. 3), more related to the roller and, in this case, instead of the vectors $\mathcal{QT}$ and $\mathbf{u\gamma}$, the followings will be used:

$$\mathbf{FT} = \begin{pmatrix} F_\xi & F_\mu & T_\zeta \end{pmatrix}^{\mathrm{T}} \tag{11}$$

$$\mathbf{u\theta} = \begin{pmatrix} u_\xi & u_\eta & \theta \end{pmatrix}^{\mathrm{T}} \tag{12}$$

where u_ξ and u_η are the displacements along the respective axis and θ is the rotation angle of the around the local axis ζ. Because the displacements are usually small, the displacement vectors $\mathbf{u\theta}$ and $\boldsymbol{\delta\theta}$ can be related:

$$\mathbf{u\theta} = \mathbf{T}_{xyz2\xi\eta\zeta}(\mathrm{O}_i, \varphi) \cdot \boldsymbol{\delta\theta} \tag{13}$$

where the transformation matrix $\mathbf{T}_{xyz2\xi\eta\zeta}(\mathrm{O}_i, \varphi)$ is given by the equation:

$$\begin{aligned} &\mathbf{T}_{xyz2\xi\eta\zeta}(\mathrm{O}_i, \varphi) = \\ &= \begin{pmatrix} \cos(\alpha-\beta) & -\sin(\alpha-\beta) & 0 \\ \sin(\alpha-\beta) & \cos(\alpha-\beta) & 0 \\ 0 & 0 & 1 \end{pmatrix} \begin{pmatrix} 1 & 0 & 0 & r_{O_i}\sin\varphi & -r_{O_i}\cos\varphi \\ 0 & \cos\varphi & \sin\varphi & -x_{O_i}\sin\varphi & x_{O_i}\cos\varphi \\ 0 & 0 & 0 & -\sin\varphi & \cos\varphi \end{pmatrix} \end{aligned} \tag{14}$$

The rolling element force vector **FT** is transformed to an equivalent force vector **fm** at the inner ring reference point:

$$\mathbf{fm} = \mathbf{T}_{\xi\eta\zeta 2xyz}(\mathrm{O}_i, \varphi) \cdot \mathbf{FT} \tag{15}$$

$$\mathbf{T}_{\xi\eta\zeta 2xyz}(\mathrm{O}_i, \varphi) = \left[\mathbf{T}_{xyz2\xi\eta\zeta}(\mathrm{O}_i, \varphi)\right]^{\mathrm{T}}. \tag{16}$$

In this point of the present approach a sub-problem can be stated as follows: If a certain vector of the inner ring displacement is given, the question is: which are the resistant loads and moments (issued by the deformation of the rollers) that acts on the inner ring? For this purpose, all the elastic forces by which all the deformed rollers, being in equilibrium, load the inner ring have to be summated. In this context, the study of the equilibrium of a certain roller is mandatory.

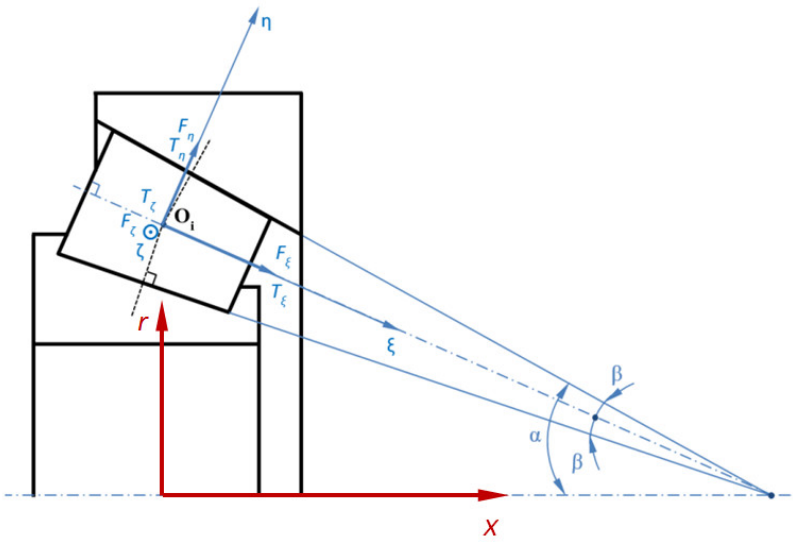

Fig. 3 – Bearing roller Cartesian coordinate systems.

In the following, some geometrical parameters of the tapper roller are presented succinctly (most of them can be observed in Fig. 4 and in the following figures):

$$\lambda = \operatorname{asin}\left(\frac{D_{\max}}{2R_{f1}}\right) \tag{17}$$

$$\beta = \operatorname{atan}\left(\frac{D_{\max} - D_{\min}}{2L}\right) \tag{18}$$

$$D_{we} = \frac{D_{\max} + D_{\min}}{2} \tag{19}$$

$$\xi_{f1} = R_{f1}\cos\lambda + \frac{D_{we}}{2}\tan\beta - \frac{L}{2} \tag{20}$$

$$R_{ap} = \frac{D_{we}}{2\cos\beta} \tag{21}$$

$$L_{we} = \frac{L - 2r_c}{\cos\beta} \tag{22}$$

where: $D_{\min}$, $D_{\max}$, and D_{we} are the minimum, maximum, and mean dimeters of the roller, L is its length (neglecting the height of the spherical end), β is the (semi)angle of the taper roller, r_c is the axial dimension of the chamfers, L_{we} is the useful length of the roller profile, R_{f1} and ξ_{f1} are the radius and the abscissa of the centre of the spherical end of roller, and λ is its angle (see Fig. 4).

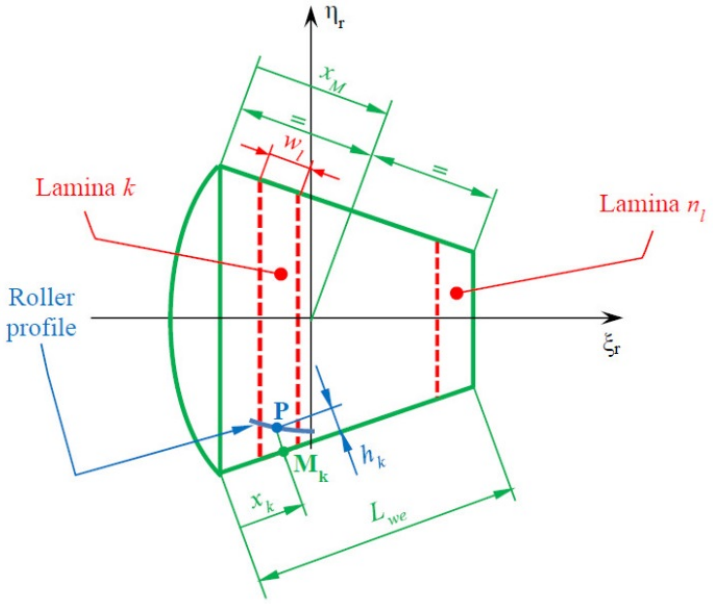

Fig. 4 – Roller laminae.

The roller is sliced (perpendicular to roller axis) in n_l (odd number) laminae and therefore one can define:

$$w_l = \frac{L_{we}}{n_l} \tag{23}$$

$$x_k = \left(k - \frac{1}{2}\right) w_l ; \quad k = 1, \ldots, n_l \tag{24}$$

$$x_M = \frac{L_{we}}{2} \tag{25}$$

$$\Delta x_k = x_k - x_M = \left(k - \frac{n_l + 1}{2}\right) w_l ; \quad k = 1, \ldots, n_l \tag{26}$$

$$h_k = P(x_k); \quad k = 1, \ldots, n_l \tag{27}$$

$$\Delta h_k = R_{ap} - h_k \tag{28}$$

where: w_l is the width of a lamina, x_k and x_M represent the coordinates of the lamina k and of the central lamina, respectively, h_k is the drop of the roller profile corresponding to the lamina k. Note that roller profile as a function of the lamina coordinate is denoted here by P. Even this topic is beyond the subject of this paper, it is worth noting here that RKB Bearing Industries, the main sponsor of this research, uses for P a special logarithmic profile, different than that recommended by the ISO 16281: 2008 [23].

In Fig. 5 the plane defined by the system of coordinates $\xi\eta$ (Fig. 3) is once again considered. Another two systems of coordinates will be introduced: $\xi_r\eta_r$, connected to the roller, and $\xi_w\eta_w$, jointly with a certain raceway (belonging to the inner ring or outer ring as well). Initially, all these three systems of coordinates coincide, and afterwards both roller and raceway move in different positions and consequently the systems move accordingly. The final position of the roller system $\xi_r\eta_r$ is given by the vector $\mathbf{t}_r\boldsymbol{\tau}_{\gamma_r}$ and rotation angle α_r. Similarly, the final position of the raceway system $\xi_w\eta_w$ is given by the vector $\mathbf{t}_w\boldsymbol{\tau}_{\gamma_w}$ and rotation angle α_w.

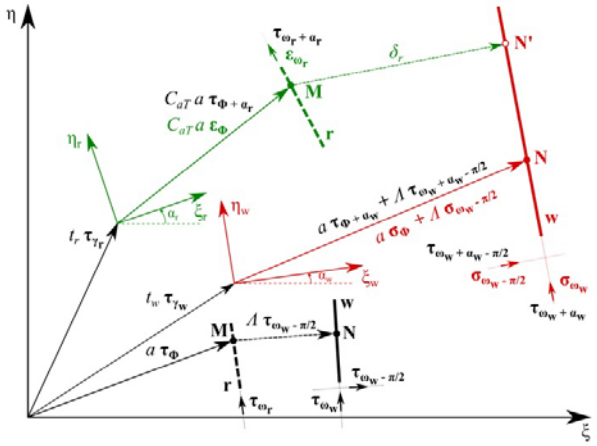

Fig. 5 – Roller generatrix and raceway before and after the movements.

The following conventions were made:

1. The letters in bold (and non-italic) are versors.
2. The other letters represent scalars.
3. In the fixed system $\xi\eta$ the versors are always denoted by $\boldsymbol{\tau}$, in the roller system by $\boldsymbol{\varepsilon}$, and in the raceway system by $\boldsymbol{\sigma}$.
4. In a certain system, the index of a versor represents the angle between the direction of the versor and the positive direction of axis of abscises (ξ, ξ_r, or ξ_w, respectively). For example, in the fixed system $\xi\eta$, the versor $\boldsymbol{\tau}_{\gamma_r}$ means $(\cos\gamma_r \quad \sin\gamma_r)^{\mathrm{T}}$.

The roller generatrix is represented by thick dash-line (versor $\boldsymbol{\tau}_{\omega_r}$) and the considered raceway by thick plain line (versor $\boldsymbol{\tau}_{\omega_w}$, almost always equals to $\boldsymbol{\tau}_{\omega_r}$). M is the reference point of the roller generatrix. In this point the drop of the profile is zero. The initial distance between the point M from the roller generatrix and the considered raceway is Λ. At the beginning, the position of point M is given by the position vector $a\boldsymbol{\tau}_\Phi = a\boldsymbol{\varepsilon}_\Phi = a\boldsymbol{\sigma}_\Phi$. After the movement of the roller (looking for the equilibrium position during its deformation), the position of point M is given by the vector $C_{aT}a\boldsymbol{\tau}_{\Phi+\alpha_r}$ (in the system $\xi\eta$), or by $C_{aT}a\boldsymbol{\varepsilon}_\Phi$ (in the roller system $\xi_r\eta_r$). Here C_{aT} is a factor that takes into account the modification of the distance a due to the variation of the roller temperature in relation to the raceway temperature.

Initially, M points toward N from the raceway ($\mathrm{MN} = \Lambda$) and after the movements of the roller and raceway, the new position of M points toward N'. Therefore, the distance between the point M and the raceway, after the movements of the roller and raceway, is given by the equation:

$$\begin{aligned}\delta_r = {} & (t_{w\xi} - t_{r\xi})\sin(\omega_w + \alpha_w) - (t_{w\eta} - t_{r\eta})\cos(\omega_w + \alpha_w) + \\ & + a\left[\sin(\omega_w - \Phi) - C_{aT}\sin(\omega_w - \Phi + \alpha_w - \alpha_r)\right] + \Lambda.\end{aligned} \tag{29}$$

It worth to be mentioned here that the model described so far is general and does not take in consideration the shape of the roller. That means the model can be used for all types of rollers (taper, cylindrical, etc.). In all cases, the final distance between the reference point of the roller generatrix and raceway is used in the calculation of the distance between a certain point of the roller profile and raceway (i.e. the distance between a roller lamina and raceway). If this distance is negative (i.e. interference) an elastic force is generated.

In the present approach, the above model is used to find the distances between the reference points of a taper roller and the raceways of the rings and large rib of the inner ring, respectively, after their movements. The initial position of the roller, raceways, and rib is presented in Fig. 6, and the input data and denotations are given in Table 1 and Table 2. The model is used both in the

preloading phase of the bearing arrangement at mounting and in the functioning phase as well. At the preloading, according to the arrangement type, $\chi = \theta = 0$ and either $s_\xi = s_\eta = 0$, or $u_\xi = u_\eta = 0$ (the other movements being nonzero). During the working phase, it is more likely that $s_\xi = s_\eta = \chi = 0$, and u_ξ, u_η, θ are nonzero being the results of the inner ring movement under the external loading. In all cases ν_ξ, ν_η and ψ are the unknowns.

Since all the rotation angles are obviously very small, in all equations that follow, the usual approximations were made: sinus and cosines of an angle were approximate by the value of the angle and 1, respectively.

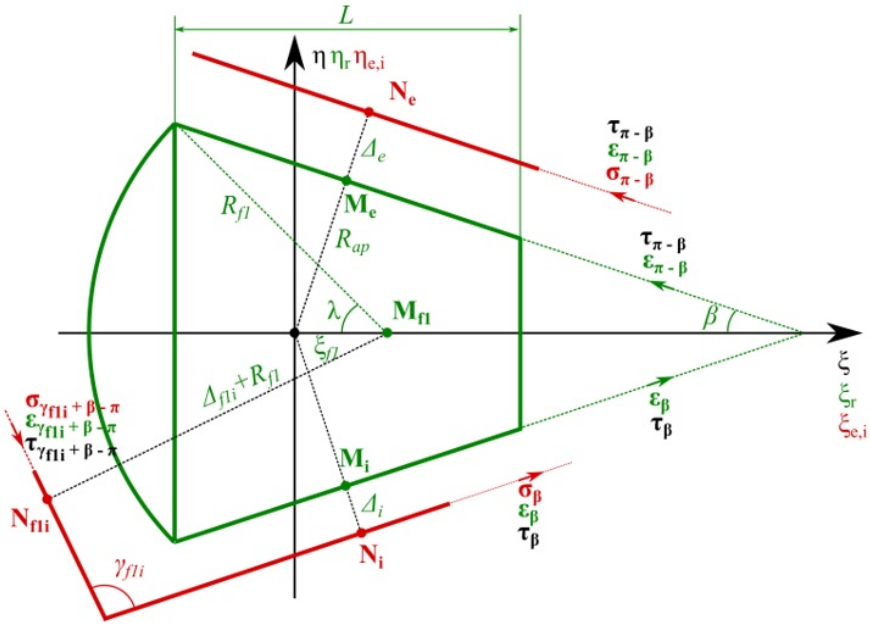

Fig. 6 – Roller, inner and outer ring raceways, and large rib of the inner ring in the initial position.

Table 1

Roller reference points-raceways distances. Input data: angles and distances

Contact between	ω_w	a	Φ	$\Lambda^{*)}$
Roller generatrix and outer ring raceway	$\pi - \beta$	R_{ap}	$\frac{\pi}{2} - \beta$	Δ_e
Roller generatrix and inner ring raceway	β	R_{ap}	$-\frac{\pi}{2} + \beta$	Δ_i
Roller spherical end and large rib of the inner ring	$\gamma_{f1i} + \beta - \pi$	ξ_{f1}	0	$R_{f_1} + \Delta_{f1i}$

*) – initial position given by Δ_e, Δ_i, and Δ_{fli} should reflect the preloading of the bearing and the expansion of rings at mounting.

Table 2

Roller reference points-raceways distances. Input data: movements (denotations)

Movement of	$t_{w\xi}$	$t_{w\eta}$	α_w	$t_{r\xi}$	$t_{r\eta}$	α_r
Outer ring	s_ξ	s_η	χ	-	-	-
Inner ring	u_ξ	u_η	θ	-	-	-
Roller	-	-	-	ν_ξ	ν_η	ψ

With all these, the equations of the distances between the reference points of the roller and the mating surfaces, after their movements, are given bellow.

Distance between the reference point of the roller generatrix and outer ring raceway:

$$\delta_e = (s_\xi - \nu_\xi)(\sin\beta - \chi\cos\beta) + (s_\eta - \nu_\eta)(\cos\beta + \chi\sin\beta) + R_{ap}(1 - C_{Tr}) + \Delta_e . \quad (30)$$

Distance between the reference point of the roller generatrix and inner ring raceway:

$$\delta_i = (u_\xi - \nu_\xi)(\sin\beta + \theta\cos\beta) - (u_\eta - \nu_\eta)(\cos\beta - \theta\sin\beta) + R_{ap}(1 - C_{Tr}) + \Delta_i . \quad (31)$$

Distance between the reference point of the roller spherical end and inner ring large rib:

$$\begin{aligned}\delta_{f1i} = &-(u_\xi - \nu_\xi)\left[\sin(\gamma_{f1i} + \beta) + \theta\cos(\gamma_{f1i} + \beta)\right] + \\ &+ (u_\eta - \nu_\eta)\left[\cos(\gamma_{f1i} + \beta) - \theta\sin(\gamma_{f1i} + \beta)\right] - \\ &- \xi_{f1}\left[(1 - C_{Tr})\sin(\gamma_{f1i} + \beta) - C_{Tr}(\theta - \psi)\cos(\gamma_{f1i} + \beta)\right] + \Delta_{f1i}. \quad (32)\end{aligned}$$

Here C_{Tr} is a generic factor that takes into account the modification of the distances due to the variation of the roller temperature in relation to the raceway temperature variation. Note also that in the following equations, in order to take into account the thermal effect, x_k, x_M, h_k are multiplied by C_{Tr}.

In Fig. 7 the relative position, after movement, of the outer ring raceway against the roller is presented. The initial position of the raceway is drawn with thick dash-line. The distance from any point P of the roller profile (defined by the coordinate x_k, corresponding to the lamina k) to the outer ring raceway can be calculated with the equation:

$$\delta e_k = \delta_e + h_k - \Delta x_k(\psi - \chi) \quad (33)$$

Obviously, if the value of the distance $\delta e_k < 0$ then an interference occurs and an elastic force is developed. Generally, the value of the elastic force is given by the following non-linear equation:

$$qe_k = c_{we}\left[\max(0, -\delta e_k)\right]^{10/9}, \tag{34}$$

where c_{we} is the spring constant of a lamina of the rolling element with line contact and it is calculated according to ISO/TS 16281: 2008(E). The total load, considering all laminae, that acts on the roller due to its contact with the outer ring raceway is:

$$Qe = \sum_{k=1}^{n_l} qe_k \ . \tag{35}$$

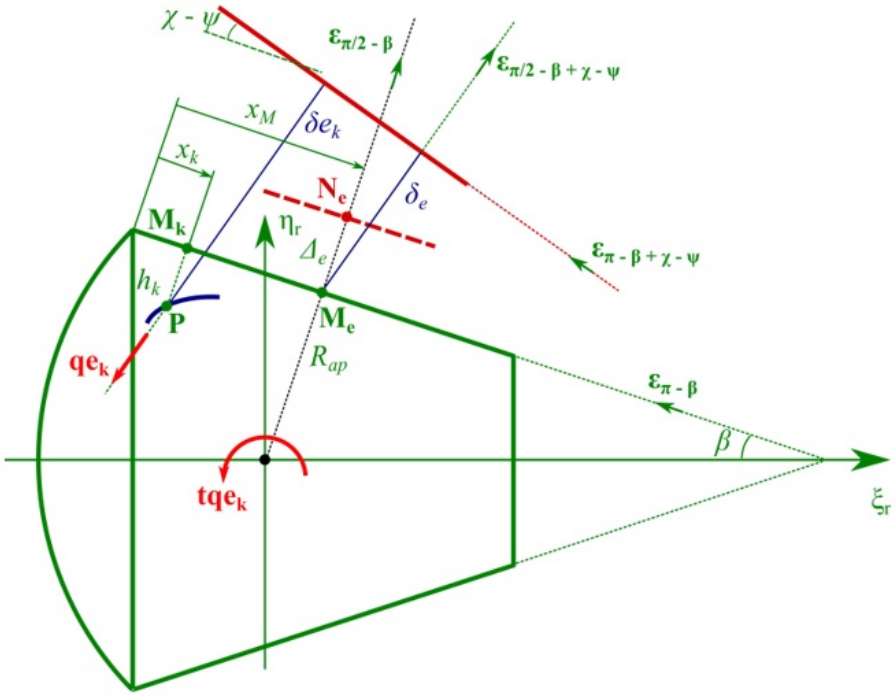

Fig. 7 – Loading of the roller by the outer ring.

The lamina load qe_k generates on the roller a moment:

$$tqe_k = qe_k\left[\Delta h_k(\psi - \chi) - \Delta x_k\right] \tag{36}$$

and the total moment (as a sum of all lamina moments) is:

$$TQe = \sum_{k=1}^{n_l} tqe_k \ . \tag{37}$$

In the roller system of coordinates, the vectors of the total load and the total moment (acting on the roller) coming from the outer ring raceway have the following equations:

$$\mathbf{Qe} = Qe\begin{pmatrix} -\sin\beta - (\psi - \chi)\cos\beta \\ -\cos\beta + (\psi - \chi)\sin\beta \\ 0 \end{pmatrix} \tag{38}$$

$$\mathbf{TQe} = TQe\begin{pmatrix} 0 \\ 0 \\ 1 \end{pmatrix} \tag{39}$$

In Fig. 8 the positions, after movement, of the inner ring raceway and the roller are represented.

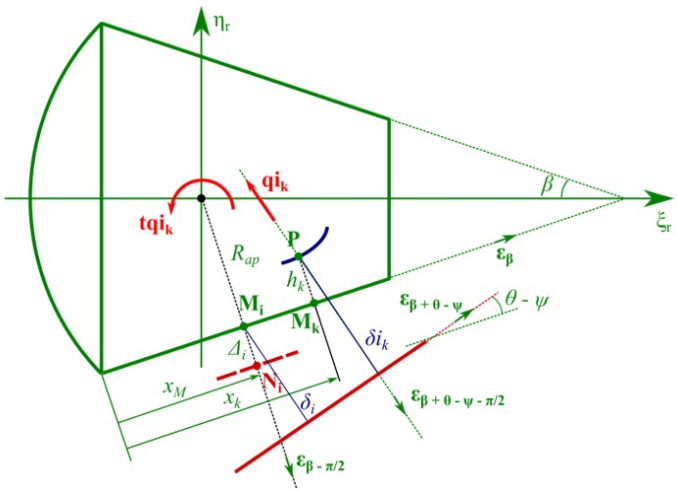

Fig. 8 – Loading of the roller by the inner ring.

The distance from any point P of the roller profile (defined by the coordinate x_k corresponding to the lamina k) to the inner ring raceway can be obtained with the equation:

$$\delta i_k = \delta_i + h_k - \Delta x_k(\theta - \psi)\,. \tag{40}$$

As in precedent case the compressive load acting on the lamina k of the roller is given by the equation

$$qi_k = c_{wi}\left[\max(0, -\delta i_k)\right]^{10/9} \tag{41}$$

and the total load with which the inner ring raceway compress the roller becomes:

$$Qi = \sum_{k=1}^{n_l} qi_k \ . \tag{42}$$

In this case, the lamina load generates a lamina moment, also:

$$tqi_k = qi_k \left[-\Delta h_k (\theta - \psi) + \Delta x_k \right] \tag{43}$$

and the total moment (as a sum of all lamina moments) is:

$$TQ_i = \sum_{k=1}^{n_l} tqi_k . \tag{44}$$

In the roller system of coordinates, the vectors of the total load and the total moment (acting on the roller) coming from the inner ring raceway are given by the following equations:

$$\mathbf{Qi} = Qi \begin{pmatrix} -\sin\beta - (\theta - \psi)\cos\beta \\ \cos\beta - (\theta - \psi)\sin\beta \\ 0 \end{pmatrix} \tag{45}$$

$$\mathbf{TQi} = TQi \begin{pmatrix} 0 \\ 0 \\ 1 \end{pmatrix} \tag{46}$$

In Fig. 9 the positions, after movement, of the inner ring large rib and the roller are presented.

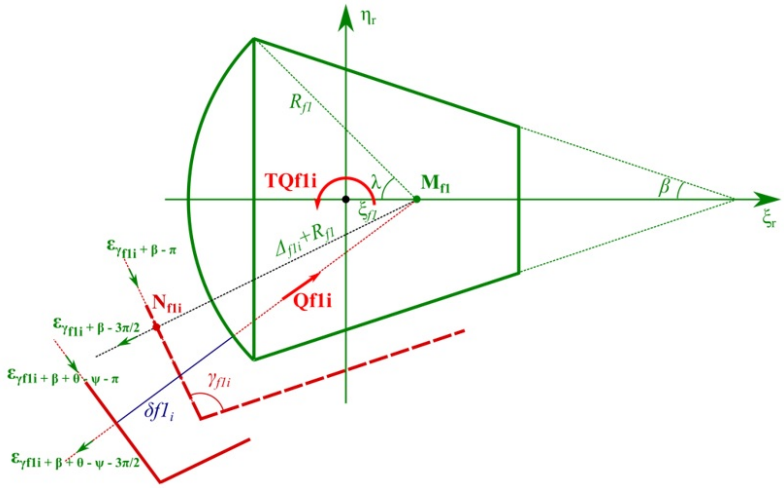

Fig. 9 – Loading of the roller by the large rib of the inner ring.

The interference (or clearance) between the spherical end of the roller and the large rib of the inner ring can be now easily computed (32):

$$\begin{aligned}\delta_{f1i} = &-(u_\xi - \nu_\xi)\left[\sin(\gamma_{f1i}+\beta)+\theta\cos(\gamma_{f1i}+\beta)\right]+\\ &+(u_\eta - \nu_\eta)\left[\cos(\gamma_{f1i}+\beta)-\theta\sin(\gamma_{f1i}+\beta)\right]-\\ &-\xi_{f1}\left[(1-C_{Tr})\sin(\gamma_{f1i}+\beta)-C_{Tr}(\theta-\psi)\cos(\gamma_{f1i}+\beta)\right]+\Delta_{f1i}\end{aligned} \tag{47}$$

In the case of interference, the elastic load that compress the roller is:

$$Qf1i = c_{Pf1i}\left[\max(0,-\delta f1_i)\right]^{3/2} \tag{48}$$

where c_{Pf1i} is the spring constant of the rolling element with point contact and is calculated according to ISO/TS 16281: 2008(E). This load will produce, obviously, a moment:

$$TQf1i = -Qf1i\,\xi_{f1}\left[\cos(\gamma_{f1i}+\beta)-(\theta-\psi)\sin(\gamma_{f1i}+\beta)\right]. \tag{49}$$

In the roller system of coordinates, the vectors of the total load and the total moment (acting on the roller) coming from the large rib of the inner ring are:

$$\mathbf{Qf1i} = Qf1i\begin{pmatrix}\sin(\gamma_{f1i}+\beta)+(\theta-\psi)\cos(\gamma_{f1i}+\beta)\\ -\cos(\gamma_{f1i}+\beta)+(\theta-\psi)\sin(\gamma_{f1i}+\beta)\\ 0\end{pmatrix} \tag{50}$$

$$\mathbf{TQf1i} = TQf1i\begin{pmatrix}0\\0\\1\end{pmatrix}. \tag{51}$$

Now it is possible to write the equations that describe the static equilibrium of the roller:

$$\begin{cases}Q_e\left[-\sin\beta-(\psi-\chi)\cos\beta\right]+Q_i\left[-\sin\beta-(\theta-\psi)\cos\beta\right]+\\ \qquad +Qf1i\left[\sin(\gamma_{f1i}+\beta)+(\theta-\psi)\cos(\gamma_{f1i}+\beta)\right]=0\\ Q_e\left[-\cos\beta+(\psi-\chi)\sin\beta\right]+Q_i\left[\cos\beta-(\theta-\psi)\sin\beta\right]+\\ \qquad +Qf1i\left[-\cos(\gamma_{f1i}+\beta)+(\theta-\psi)\sin(\gamma_{f1i}+\beta)\right]=0\\ TQE+TQi+TQf1i=0\end{cases} \tag{52}$$

The unknowns of the system of equations (52) are ν_ξ, ν_η, ψ and they describe the final position of the roller when it reaches the static equilibrium

position. The non-linear system of equations (52) must be solved for each roller of the bearing and with the solutions of each roller apart, the loads and moments that act on the inner ring can be calculated with the equation:

$$\mathbf{FT}_j = \begin{pmatrix} Q_i\left[\sin\beta + (\theta-\psi)\cos\beta\right] + Qf1i\left[-\sin(\gamma_{f1i}+\beta) - (\theta-\psi)\cos(\gamma_{f1i}+\beta)\right] \\ Q_i\left[-\cos\beta + (\theta-\psi)\sin\beta\right] + Qf1i\left[\cos(\gamma_{f1i}+\beta) - (\theta-\psi)\sin(\gamma_{f1i}+\beta)\right] \\ -TQi - TQf1i \end{pmatrix}_j \quad (53)$$

where $j = 1, 2, \ldots, Z$ and Z is the number of the rollers. The rolling element force vector $\mathbf{FT}_j$ is transformed to an equivalent force vector $\mathbf{fm}_j$ at the inner ring reference point by using equation (15).

$$\mathbf{fm}_j = \mathbf{T}_{\xi\eta\zeta 2xyz}(\mathrm{O}_i, \varphi_j) \cdot \mathbf{FT}_j . \quad (54)$$

Finally, the loading from all the rolling elements on the inner ring, in the bearing reference point is:

$$\mathfrak{fm} = \sum_{j=1}^{z} \mathbf{fm}_j \quad (55)$$

and, consequently, the corresponding loadings in the considered nodes k_1 and k_2 are $\mathfrak{fm}_{k_1}$ and $\mathfrak{fm}_{k_2}$, respectively. These two vectors can be easily aggregate in a single vector representing, in fact, the reactions of the bearings to the external forces and moments that load the shaft:

$$\mathbf{fm} = \left(\mathfrak{f}_x \quad \mathfrak{f}_{y_{k1}} \quad \mathfrak{f}_{z_{k1}} \quad \mathfrak{m}_{y_{k1}} \quad \mathfrak{m}_{z_{k1}} \quad \mathfrak{f}_{y_{k2}} \quad \mathfrak{f}_{z_{k2}} \quad \mathfrak{m}_{y_{k2}} \quad \mathfrak{m}_{z_{k2}}\right)^{\mathrm{T}} \quad (56)$$

where

$$\mathfrak{f}_x = \mathfrak{f}_{x_{k1}} + \mathfrak{f}_{x_{k2}} . \quad (57)$$

4. BEARING ARRANGEMENT LIFE

Due to static equilibrium, the sum of the loads/moments transmitted from the shaft to the bearings and the loads/moments transmitted to the shaft due to the bearing elastic deformations must be zero. This leads to the equation:

$$\mathbf{FM} + \mathbf{fm} = 0 \quad (58)$$

which is in fact a system of nine nonlinear equations with nine unknowns (the components of the vector $\Delta\Theta$) and the unknowns must be generally solved by

iteration. Once the vector $\boldsymbol{\Delta\Theta}$ is known, it can be decomposed into the two vectors $\boldsymbol{\delta\theta}_{k_1}$ and $\boldsymbol{\delta\theta}_{k_2}$, corresponding to the two bearing reference points:

$$\boldsymbol{\delta\theta}_{k_1} = \left(\delta_x \quad \delta_{y_{k1}} \quad \delta_{z_{k1}} \quad \theta_{y_{k1}} \quad \theta_{z_{k1}}\right)^{\mathrm{T}} \tag{59}$$

$$\boldsymbol{\delta\theta}_{k_2} = \left(\delta_x \quad \delta_{y_{k2}} \quad \delta_{z_{k2}} \quad \theta_{y_{k2}} \quad \theta_{z_{k2}}\right)^{\mathrm{T}}. \tag{60}$$

In the following, to ease the presentation, the sub-scripts k_1 and k_2 will be omitted, meaning that, for both nodes, the same calculation will be done starting with a certain vector $\boldsymbol{\delta\theta}$. For every roller, the following steps have to be done:

1. The displacement vectors $\mathbf{u\theta}_j$ are calculated using equation (13):

$$\mathbf{u\theta}_j = \mathbf{T}_{xyz2\xi\eta\zeta}(\mathrm{O}_i, \varphi_j) \cdot \boldsymbol{\delta\theta}; \tag{61}$$

2. The distance between the reference point of the roller generatrix and the outer ring raceway is calculated using equation (30). Note that, during the functioning, one can consider $s_\xi = s_\eta = 0,\ \chi = 0$:

$$\delta_{e_j} = -\nu_{\xi_j} \sin\beta - \nu_{\eta_j} \cos\beta + R_{ap}(1 - C_{Tr}) + \Delta_e; \tag{62}$$

3. The distances between each point of profile lamina and the outer ring raceway are computed using equation (33):

$$\delta e_{j,k} = \delta_{e_j} + h_k - \psi_j \Delta x_k; \tag{63}$$

4. The values of the compressive elastic forces, acting on each lamina, are obtained using the non-linear equation (34):

$$qe_{j,k} = c_{we}\left[\max(0, -\delta e_{j,k})\right]^{10/9}; \tag{64}$$

5. The distance between the reference point of the roller generatrix and the inner ring raceway is calculated by means of the equation (31):

$$\delta_{i_j} = \left[(u_\xi - \nu_\xi)_j(\sin\beta + \theta_j \cos\beta) - (u_\eta - \nu_\eta)_j(\cos\beta - \theta_j \sin\beta) + R_{ap}(1 - C_{Tr}) + \Delta_i\right] \tag{65}$$

6. The distances between each point of profile lamina and the inner ring raceway are computed using equation (40):

$$\delta i_{j,k} = \delta_{i_j} + h_k - \Delta x_k(\theta_j - \psi_j); \tag{66}$$

7. The values of the compressive elastic forces, acting on each lamina, are obtained using the non-linear equation (41):

$$qi_{j,k} = c_{wi}\left[\max(0, -\delta i_{j,k})\right]^{10/9}. \tag{67}$$

Now, the values of the loads that compress each lamina of each roller – given by the equations (64) and (67) – must be used in bearing life calculation according to the newest ISO/TS 16281. The obtained lives of the two bearings should now aggregated in the bearing arrangement life (according to the product low [16], as the life of a multi-row bearing is calculated).

$$L_{arr} = \left(L_1^{-9/8} + L_2^{-9/8}\right)^{-8/9} \tag{68}$$

where L_1 and L_2 are the bearing rating lives (basic or modified) and L_{arr} is the corresponding rating life of the bearing arrangement.

Note that this rating life will be the objective function of the further proposed optimization.

5. CONCLUSIONS

The first part of this paper provides a new bearing load calculation method. The static equilibrium of the shaft is attained when the loads and moments transmitted from the shaft to the bearings are reacted by the loads and moments arisen due to the elastic deformations of the rolling elements. Using the slope-deflection method and taking into account the shaft material, geometry and loading, the loads and moments transmitted to the bearings are expressed as a function of shaft deflections and rotation at reference supporting points.

The simplicity of the method converts this approach into a versatile and reliable one. The reactions and moment reactions were expressed as function of the same unknowns using a dynamic model. The unknowns are determined first by solving the equations of equilibrium. Once the displacements are known, the unknown compressive forces among the bearing rolling elements are obtained from the accepted bearing dynamic model.

The subsequent parts of the paper highlight the application of the proposed method to the life calculations of the bearings from particular real-world bearing arrangements whereas in the last part, the optimal design of such bearing arrangement (from the perspective of the maximum bearing arrangement life) is rendered.

Acknowledgments. The authors would like to thank the RKB Group, the Swiss bearing manufacturer, for the permission to publish these results and the RKB staff for their great interest and support during the development of this project.

Received on October 15, 2017

REFERENCES

1. ANDREASON, S., *Theoretische Grundlagen fur die Berechnung von mit Kraften und Momenten belasteten Rillenkugellagern*, Konstruktion, pp. 105–109, 1969.
2. BAI, C., XU, Q., *Dynamic model of ball bearings with internal clearance and waviness*, Journal of Sound and Vibration, **294**, *1–2*, pp. 23–48, 2006.
3. BAI, C., ZHANG, H., XU, Q., *Effects of axial preload of ball bearing on the nonlinear dynamic characteristics of a rotor-bearing system*, Nonlinear Dynamics, **53**, *3*, pp. 173–190, 2008.
4. BENDIXSEN, A., *Die Methode der Alpha-Gleichungen zur Berechnung von Rahmenkonstruktionen* (The method of alpha equations for the calculation of frame structures), Springer, 1914.
5. CONNOR, J.J., FARAJI, S., *Fundamentals of Structural Engineering*, Springer, 2013.
6. CRETU, S., BERCEA, I., MITU, N., *A dynamic analysis of tapered roller bearing under fully flooded conditions. Part 1: Theoretical formulation*, Wear, **188**, *1–2*, pp. 1–10, 1995.
7. DE MUL, J.M., VREE, J.M., MAAS, D.A., *Equilibrium and associated load distribution in ball and roller bearings loaded in five degrees of freedom while neglecting friction. Part I: General theory and application to ball bearings*, Journal of Tribology – Transactions of the ASME, **111**, *1*, pp. 142–148, 1989.
8. DE MUL, J.M., VREE, J.M., MAAS, D.A., *Equilibrium and associated load distribution in ball and roller bearings loaded in five degrees of freedom while neglecting friction. Part II: Application to roller bearings and experimental verification*, Journal of Tribology – Transactions of the ASME, **111**, *1*, pp. 149–155, 1989.
9. GARGIULO Jr., E.P., *A simple way to estimate bearing stiffness*, Machine Design, **52**, *7*, pp. 107–110, 1980.
10. GUNDUZ, A., *Multi-dimensional stiffness characteristics of double row angular ball bearings and their role in influencing vibration modes*, Ph.D. Thesis, The Ohio State University, 2012.
11. GUO, Y., PARKER, R.G., *Stiffness matrix calculation of rolling element bearings using a finite element/contact mechanics model*, Mechanism and Machine Theory, **51**, pp. 32–45, 2012.
12. GUPTA, P.K., *Dynamics of rolling-element bearings. Part I: Cylindrical roller bearing analysis*, Journal of Lubrication Technology – Transaction of the ASME, **101**, *3*, pp. 293–302, 1979.
13. GUPTA, P.K., *Dynamics of rolling-element bearings. Part II: Cylindrical roller bearing results*, Journal of Lubrication Technology – Transaction of the ASME, **101**, *3*, pp. 305–311, 1979.
14. GUPTA, P.K., *Dynamics of rolling-element bearings. Part III: Ball bearing analysis*, Journal of Lubrication Technology – Transaction of the ASME, **101**, *3*, pp. 312–318, 1979.
15. GUPTA, P.K., *Dynamics of rolling-element bearings. Part IV: Ball bearing results*, Journal of Lubrication Technology – Transaction of the ASME, **101**, *3*, pp. 319–326, 1979.
16. HARRIS, T.A., KOTZALAS, M.N., *Rolling bearing analysis: Essential concepts of bearing technology*, Taylor & Francis/CRC Press, 2007.
17. HARRIS, T.A., KOTZALAS, M.N., *Rolling bearing analysis: Advanced concepts of bearing technology*, Taylor & Francis/CRC Press, 2007.
18. HERNOT, X., SARTOR, M., GUILLOT, J., *Calculation of the stiffness matrix of angular contact ball bearings by using the analytical approach*, Journal of Mechanical Design, **122**, *1*, pp. 83–90, 2000.
19. HIBBELER, R.C., *Structural Analysis*, 8th edition, Prentice Hall, 2012.
20. HOUPERT, L., *A uniform analytical approach for ball and roller bearings calculations*, Journal of Tribology – Transaction of the ASME, **119**, *4*, pp. 851–858, 1997.
21. HOUPERT, L. *An enhanced study of the load-displacement relationships for rolling element bearings*, Journal of Tribology – Transaction of the ASME, **136**, *1*, pp. 1–11, 2014.
22. International Organization for Standardization, *Rolling bearings – Dynamic load ratings and rating life*, ISO 281: 2007(E).
23. International Organization for Standardization, *Rolling bearings – Methods for calculating the modified reference rating life for universally loaded bearings*, ISO/TS 16281: 2008(E).

24. JONES, A.B., *Analysis of stresses and deflections*, Technical Report NREL/TP-500-36881, Vol. 1 and 2, New Departure Division, General Motors Corp., Bristol, Connecticut, 1946.
25. JONES, A.B., *A general theory for elastically constrained ball and radial roller bearings under arbitrary load and speed conditions*, Journal of Basic Engineering, pp. 309–320, 1960.
26. KARNOVSKY, I.A., LEBED, O., *Advanced methods of structural analysis*, Springer, 2010.
27. LIAO, N.T., LIN, J.F., *A new method for the analysis of deformation and load in a ball bearing with variable contact angle*, Journal of Mechanical Design – Transaction of the ASME, **123**, *2*, pp. 304–312, 2001.
28. LIAO, N.T., LIN, J.F., *Ball bearing skidding under radial and axial loads*, Mechanism and Machine Theory, **37**, *1*, pp. 91–113, 2002.
29. LIEW, J.Y.R., SHANMUGAM, N.E., *Theory and analysis of structures*, in: *The Civil Engineering Handbook*, 2nd edition (Eds. W.F. Chen, J.Y.R. Liew), CRC Press, 2003.
30. LIM, T.C., SINGH, R., *Vibration transmission through rolling element bearings. Part I: Bearing stiffness formulation*, Journal of Sound and Vibration, **139**, *2*, pp. 179–199, 1990.
31. LIN, C.-W., LIN, Y.-K., CHU, C.-H., *Dynamic models and design of spindle-bearing systems of machine tools: A review*, International Journal of Precision Engineering and Manufacturing, **14**, *3*, pp. 513–521, 2013.
32. MANDERLA, H., *Die Berechnung der Sekundärspannungen, welche im einfachen Fachwerk in Folge starrer Knotenverbindungen auftreten* (The calculation of the secondary stresses which occur in simple truss with consecutive rigid joint connections), Allgemeine Bauzeitung, **45**, pp. 27–43, 1880.
33. MARTI, P., *Theory of structures. Fundamentals frame structures, plates, and shells*, Wiley, Ernst & Sohn, 2013.
34. MATHESON, J.A.L., FRANCIS, A.J., *Hyperstatic structures. An introduction to the theory of statically indeterminate structures*, Vol. II, London, Butterworth's Scientific, 1960.
35. MEGSON, T.H.G., *Structural and stress analysis*, 2nd edition, Elsevier, 2005.
36. MOHR, O., *Die Berechnung der Fachwerke mit starren Knotenverbindungen* (The calculation of trussed frameworks with rigid joint connections), Zivilingenieur, **38**, pp. 577–594, 1892 and **39**, pp. 67–78, 1893.
37. NOEL, D., LE LOCH, S., RITOU, M., FURET, B., *Complete analytical expression of the stiffness matrix of angular contact ball bearings*, Journal of Tribology – Transaction of the ASME, **135**, *4*, pp. 1–8, 2013.
38. OSWALD, F.B., ZARETSKY, E.V., POPLAWSKI, V.P., *Effect of internal clearance on load distribution and life of radially loaded ball and roller bearings*, NASA/TM–2012-217115, 2012.
39. SINGH, R., LIM, T.C., *Vibration transmission through rolling element bearings in geared rotor system*, Grant No. NAG 3-773, Final Report – Part I, RF Project 765863/719176, The Ohio State University, 1989.
40. SJOVÄLL, H., *Belastningsfördelningen inom Kul-Och Rull-Lager Vid Givna Yttre Radial-Och Axialbelastningar* (The Load Distribution within Ball and Roller Bearings under Given External Radial and Axial Load), Teknisk Tidskrift, Mek., h.9, 1933.
41. TUDOSE, L., RUSU, F., TUDOSE, C., *Optimal design under uncertainty of bearing arrangements*, Mechanism and Machine Theory, **98**, pp. 164–179, 2016.
42. WILSON. W.M., MANEY, G.A., *Wind stresses in the steel frames of office buildings*, University of Illinois Bulletin, **12**, *40*, Engineering Experiment Station, Bulletin No. 80, 1915.
43. WILSON, W.M., RICHARD, F.E., WEISS, *C., Analysis of statically indeterminate structures by the slope deflection method*, University of Illinois Bulletin, **XVI**, *10*, Engineering Experiment Station, Bulletin No. 108, 1918.